The electronic structure, and magnetic and structural properties of Fe - Cu and Fe - Ag alloys

1997 J. Phys.: Condens. Matter 9 4455

(http://iopscience.iop.org/0953-8984/9/21/011)

J. Phys.: Condens. Matter **9** (1997) 4455–4466. Printed in the UK PII: S0953-8984(97)79348-2

The electronic structure, and magnetic and structural properties of Fe–Cu and Fe–Ag alloys

S S A Razee†, R Prasad and R M Singru

Department of Physics, Indian Institute of Technology, Kanpur 208016, India

Received 7 November 1996, in final form 31 January 1997

Abstract. We present the electronic structure, magnetic properties, and structural properties of metastable $Fe_{1-x}Cu_x$ and $Fe_{1-x}Ag_x$ alloys over the whole composition range. Although in the equilibrium state (Fe, Cu) and (Fe, Ag) do not form solid solutions, recent experiments show that by using special techniques, continuous and homogeneous solid solutions of (Fe, Cu) and (Fe, Ag) can be formed over the whole concentration range. In the present work, we have used the tight-binding linear-muffin-tin-orbital method with the coherent-potential approximation to calculate the electronic structure and magnetic moment of these alloys. Our calculation of the density of states shows two very clear peaks due to Fe and Cu (Ag), in agreement with the experimental x-ray photoemission spectroscopy results. Also our calculated values of the magnetic moments for different compositions of the alloys are found to be in good agreement with the experimental results. Our calculation shows that an Fe atom in an Fe–Cu alloy has a lower magnetic moment than an Fe atom in an Fe–Ag alloy for the same composition. We have also calculated the heat of formation of these alloys, which we always find to be positive, implying the non-existence of stable phases of these alloys under equilibrium conditions.

1. Introduction

During the last decade, the electronic structure and other related properties of disordered alloys have been a subject of considerable interest, both theoretically and experimentally. Although the Korringa–Kohn–Rostoker (KKR) method combined with the coherent-potential approximation (CPA) (see, e.g., [1, 2], and references therein) is perhaps the most accurate single-site scheme for the study of electronic structure and related properties of random substitutional alloys, its linearized version, the linear-muffin-tin-orbital (LMTO) method, in the most localized or tight-binding (TB) representation [3–6], has emerged as an efficient and computationally fast method for the calculation of the electronic structure of solids without much loss of accuracy. The TB-LMTO method, like the KKR method, is a first-principles parameter-free method within the local-spin-density approximation (LSDA) of the density functional theory (DFT) [7], and its accuracy is comparable to that of the KKR method. Kudrnovsky and co-workers [8–11] have shown that the TB-LMTO method can be adopted for random disordered alloys with the incorporation of the CPA in this scheme. It has also been shown recently that one can go beyond the single-site CPA, an exercise necessary in dealing with alloys having correlated disorder such as short-range order, within the TB-LMTO scheme [12, 13].

In this paper, we present the electronic structure, and magnetic and structural properties of Fe–Cu and Fe–Ag systems, using the TB-LMTO-CPA scheme. The interest in these

† Present address: Department of Physics, University of Warwick, Coventry CV4 7AL, UK.

0953-8984/97/214455+12$19.50

systems is borne out of the following observations. Fe has a half-filled d band, whereas the d bands of Cu and Ag are well below the Fermi energy (E_F). Fe is ferromagnetic and has a bcc structure, in contrast to Cu and Ag which are paramagnetic and fcc noble metals having similar band structures. Fe has eight electrons in its outermost shell, whereas Cu and Ag both have eleven electrons in their outermost shells, and, therefore, by varying the composition of the alloy, one can vary the electron/atom ratio continuously from eight to eleven. Also, the understanding of the electronic and magnetic structure of magnetic thin films of iron alloys bears important relevance for both fundamental and applied physics [14]. For example, there has been a lot of interest in the giant magnetoresistance of Fe–Ag alloys. Also, artificially structured ferromagnetic materials, such as films and multilayers, have attracted growing attention in view of their interesting and potential future applications as magnetic materials [15, 16]. Our studies on the electronic properties of Fe–Cu and Fe–Ag alloys can be valuable in the design of their artificial structures, even though we present here their bulk electronic properties.

Unlike the case for most transition metals, which dissolve easily in noble metals, the Fe solubility in Cu and Ag is almost zero. The phase diagrams of the Fe–Cu and Fe–Ag systems indicate that they are completely immiscible in the equilibrium solid states [17, 18]. In the case of Fe–Cu, it is possible to obtain a solid solution at the terminal concentration regions by solid quenching [19, 20], but Fe and Ag are immiscible even in the liquid state [21]. However, in recent years, it has been shown that metastable and homogeneous alloys of Fe–Cu and Fe–Ag systems can be formed over the entire range of compositions by using special techniques, such as thermal evaporation [22, 23], liquid quenching [24], ion implantation [25], sputtering [21, 26–29], and high-energy ball-milling [30]. It has been reported [29] that $Fe_{1-x}Cu_x$ alloys have a single bcc phase for $0 < x < 0.4$, a mixture of bcc and fcc phases for $0.4 < x < 0.6$, and a single fcc phase for $0.6 < x < 1.0$, and that $Fe_{1-x}Ag_x$ alloys form a single bcc phase for $0 < x < 0.14$, a mixture of bcc and fcc phases for $0.14 < x < 0.6$, and a single fcc phase for $0.6 < x < 1.0$. There have been several experimental studies on these metastable alloys. The magnetic properties [21, 26–28], the Mössbauer effect [21, 31–35], and the process of phase separation during annealing at elevated temperatures [27] are extensively investigated. It has been observed that the spontaneous magnetization persists up to very low Fe concentrations in both Fe–Cu and Fe–Ag alloys [21, 26]. Also, we have found some reports on the experimental study of the electronic structure of these alloys using x-ray photoemission spectroscopy (XPS) [29, 36].

Kudrnovsky and co-workers [37, 38] have studied the electronic structure of these alloys using the TB-LMTO-CPA scheme, but their calculations were based on an approximate charge self-consistency scheme. In their work, they used atomic-sphere potentials of pure constituents, but rescaled to their equilibrium Wigner–Seitz radii in the alloy. These *frozen* atomic-sphere potentials are approximately neutral in their own spheres and are related to a common energy zero. This approach usually works quite well for paramagnetic systems, but the ferromagnetic atomic-sphere potentials are not generally transferable, as the magnetic moment and hence the level splitting can vary significantly on alloying. However, Kudrnovsky *et al* [38] have justified their use of the above approach for Fe–Cu and Fe–Ag systems by stating that the magnetic moments on the Fe atoms in these alloys remain essentially constant and close to the pure crystal value. But our calculations show that this is not so, especially in the Fe–Ag systems, in which the Fe moments vary considerably as a function of composition. Moreover, we feel that a fully self-consistent calculation is needed for the study of the magnetic and structural properties of ferromagnetic systems. In this paper, we calculate the electronic structure of these alloys from a first-principles point of view, and study the magnetic and structural properties through their electronic structure.

We present the electronic density of states (DOS) of $Fe_{1-x}Cu_x$ ($x = 0.0$, 0.17, 0.35, 0.53, 0.66, 0.90, and 1.0) and $Fe_{1-x}Ag_x$ ($x = 0.0$, 0.13, 0.25, 0.45, 0.67, 0.92, and 1.0) alloys calculated using the scalar relativistic all-electron fully charge self-consistent TB-LMTO-CPA scheme. The theoretical results are compared with the experimental XPS results of Ushida *et al* [29], and we find a good overall agreement between the two. We have also calculated the magnetic moment of these alloys throughout the entire range of compositions, and have compared our results with the available experimental results [21, 26]. We observe that though the theory slightly overestimates the value of the magnetic moment, there is a general qualitative agreement between the two. Our calculation of the heat of formation of these alloys corroborates the experimental observation that under equilibrium conditions Fe–Cu and Fe–Ag alloys cannot be formed.

The outline of this paper is as follows. In section 2, we briefly present the computational details. In section 3, we present our results; the total and spin-polarized DOS, the magnetic properties, and the alloy formation energy are presented in subsections 3.1, 3.2, and 3.3 respectively. Finally, in section 4, we summarize our results.

2. The method of calculation

The electronic structure of disordered $Fe_{1-x}Cu_x$ and $Fe_{1-x}Ag_x$ alloys was calculated using the all-electron fully charge self-consistent scalar relativistic TB-LMTO-CPA method described in detail in the literature [8–11]. The charge self-consistency is treated within the LSDA of the DFT [7]. In our calculations, we have used the parametrization of von Barth and Hedin for the exchange–correlation potential [39]. The only input parameters in our calculations are the atomic numbers of Fe ($Z = 26$), Cu ($Z = 29$), and Ag ($Z = 47$), and the lattice structure. The lattice parameters for different compositions of the alloys were taken from reference [29].

We started with atomic potentials for the components of the alloy, and constructed the Hamiltonian in the orthogonal representation within the atomic-sphere approximation. Then the TB-LMTO-CPA equations were solved to a high degree of accuracy. The $\boldsymbol{k}$-integration necessary in the calculation of the alloy Green's function was performed on a regular network of $\boldsymbol{k}$-points in the irreducible wedge of the Brillouin zone (BZ). We have divided the Γ–X edge into 14 equal parts for the fcc lattice and the Γ–H edge into 16 equal parts for the bcc lattice, which gives approximately 250 $\boldsymbol{k}$-points in the irreducible BZ in both cases. The integration method uses the complex energy plane, thereby speeding up the calculations. The desired physical quantities were then obtained by numerical analytical continuation back to the real axis [40] after the convergence had been achieved. We calculate the charge densities from the converged alloy Green's function and iterate until charge self-consistency is achieved. The level of self-consistency of the crystal potentials on the Fe, Cu, and Ag sites (i.e. the difference between the input and output potentials at each point of the radial mesh) was less than 10^{-8} Ryd. The Fermi energies converged to within 0.1 mRyd in all of the cases. Furthermore, in our calculations, we have included the effects of lattice relaxation in an approximate way *à la* Kudrnovsky and Drchal [9, 41]. The idea is to choose the atomic-sphere radii of the components in such a way that the spheres are charge neutral. The constraints are that the spheres fill all space, and that the validity of the atomic-sphere approximation is preserved.

In our calculations, the ratio of the Wigner–Seitz radii of the two components of the alloy falls between 0.98 and 1.03 for the whole composition range, which is well within the range of validity of the atomic-sphere approximation [41]. This exercise has one more advantage: since the atomic spheres are charge neutral, the Madelung contribution to the

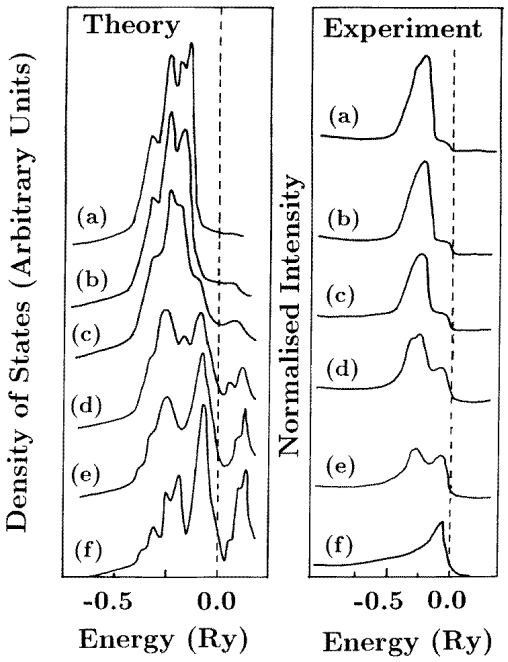

Figure 1. The total density of states (left-hand panel) of the present work, and x-ray photoemission spectra (right-hand panel) (after Ushida *et al*, reference [29]) for different constituents of the $Fe_{1-x}Cu_x$ alloy. The curves (a), (b), (c), (d), (e), and (f) correspond to the alloy constituents with $x = 1.0$, 0.90, 0.66, 0.35, 0.17, and 0.0 respectively. The vertical dotted line indicates the Fermi level.

total energy of the alloy vanishes, which makes it much simpler to calculate the total energy. The total energies of the system which we obtained in the present calculations are accurate up to 0.1 mRyd.

We have calculated the total and spin-resolved DOS for $Fe_{1-x}Cu_x$ ($x = 0.0$, 0.17, 0.35, 0.53, 0.66, 0.90, and 1.0) and $Fe_{1-x}Ag_x$ ($x = 0.0$, 0.13, 0.25, 0.45, 0.67, 0.92, and 1.0) alloys. The magnetic moment per atom of the alloy was calculated from the following relation:

$$\mu = [N_\uparrow(E_F) - N_\downarrow(E_F)]\mu_B \tag{1}$$

where $N_\uparrow(E_F)$ and $N_\downarrow(E_F)$ are respectively the integrated DOS at the Fermi energy for majority and minority spins, and μ_B is the Bohr magnetron.

The formation energy or the heat of formation of a particular composition of the alloy $Fe_{1-x}M_x$ (M = Cu or Ag) is defined as

$$\Delta H = E_{coh}(\text{alloy}) - (1-x)E_{coh}(\text{Fe}) - xE_{coh}(\text{M}) \tag{2}$$

where E_{coh}(alloy) is the cohesive energy of the alloy, and E_{coh}(Fe) and E_{coh}(M) denote the cohesive energies of elemental Fe and M (M = Cu or Ag) respectively. Since the cohesive energy of a solid is the difference between the total energy of the solid and the total energy of the isolated atoms, we can rewrite the above equation as

$$\Delta H = E_{tot}(\text{alloy}) - (1-x)E_{tot}(\text{Fe}) - xE_{tot}(\text{M}). \tag{3}$$

We have used equation (3) to calculate the heat of formation for different compositions of $Fe_{1-x}Cu_x$ and $Fe_{1-x}Ag_x$ alloys.

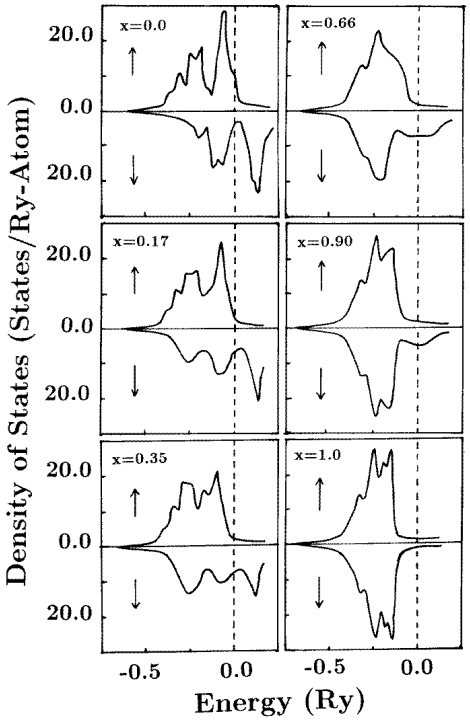

Figure 2. The spin-resolved density of states for $Fe_{1-x}Cu_x$ alloys for $x = 0.0$, 0.17, 0.35, 0.66, 0.90, and 1.0. The vertical dotted line indicates the Fermi level.

3. Results and discussion

3.1. The electronic density of states

We have calculated the spin-polarized as well as the total DOS for $Fe_{1-x}Cu_x$ ($x = 0.0$, 0.17, 0.35, 0.53, 0.66, 0.90, and 1.0) and $Fe_{1-x}Ag_x$ ($x = 0.0$, 0.13, 0.25, 0.45, 0.67, 0.92, and 1.0) alloys, using the first-principles TB-LMTO-CPA formalism. First we discuss the results for the $Fe_{1-x}Cu_x$ system. In the range $0.4 < x < 0.6$, $Fe_{1-x}Cu_x$ alloys form a mixture of bcc and fcc phases. On the Cu-rich side of this range ($x > 0.6$), these alloys have a single fcc phase, and on the Fe-rich side of this range, ($x < 0.4$) these alloys have a single bcc phase. However, Ushida *et al* [29] report that for $x = 0.53$ the dominant phase is the fcc phase. Therefore, in our calculations, we have taken a single bcc phase for $x = 0.0$, 0.17, and 0.35, and we have assumed a single fcc phase for $x = 0.53$, 0.66, 0.90 and 1.0. In figure 1 we show the total DOS for $Fe_{1-x}Cu_x$ alloys for these concentrations (left-hand panel) along with the experimental XPS results (right-hand panel).

Our calculated DOS are qualitatively similar to those reported by Kudrnovsky *et al* [38], where self-consistency was adopted in an approximate way. Although the interpretation of the XPS results would require the calculation of matrix elements, and many-body effects, convolution with the experimental resolution, and modulation by the photoionization cross section, etc [38, 42], the XPS does reflect the dominant features of the DOS, and thus our comparison should be viewed in this light. We observe that the Fermi energy in pure Fe lies around the middle of the Fe d band, while in Cu it lies well above the Cu d band. Therefore, we expect that $Fe_{1-x}Cu_x$ will form a split-band system, which is what we observe both in our theoretical results and in the XPS results of Ushida *et al* [29]. We see that as one adds Fe to Cu, a new peak in the alloy DOS emerges due to Fe. In $Fe_{65}Cu_{35}$, two

peaks are clearly visible. As the concentration of Fe increases, the Cu-derived peak gets progressively weaker, and finally disappears in pure Fe. Also, we observe that the DOS at E_F is of predominantly Fe 3d character, and as the Cu concentration increases, the Fe-derived d band in the DOS shrinks in conformity with the experimental results. In figure 2 we show the spin-resolved DOS for the above compositions of the $Fe_{1-x}Cu_x$ alloy, which also agree with the results of Kudrnovsky *et al* [38]. We observe that the d band of the majority spin is almost filled for all of the compositions, and that the main contribution to the total DOS at E_F is from the minority spin.

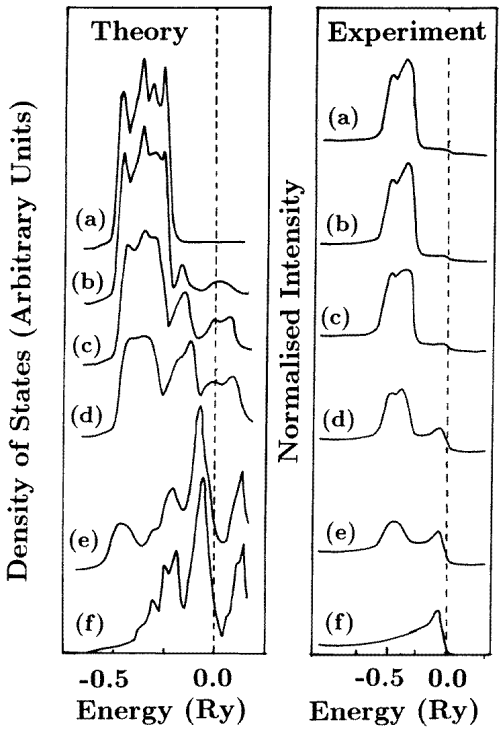

Figure 3. The total density of states (left-hand panel) of the present work, and x-ray photoemission spectra (right-hand panel) (after Ushida *et al*, reference [29]) for different constituents of the $Fe_{1-x}Ag_x$ alloy. The curves (a), (b), (c), (d), (e), and (f) correspond to the alloy constituents with $x = 1.0$, 0.92, 0.67, 0.45, 0.13, and 0.0 respectively. The vertical dotted line indicates the Fermi level.

We now present the results for $Fe_{1-x}Ag_x$ alloys. Compared with that for $Fe_{1-x}Cu_x$ alloys, the concentration range over which $Fe_{1-x}Ag_x$ alloys form a mixture of bcc and fcc phases is considerably wider, i.e. $0.14 < x < 0.6$. For $x < 0.14$, these alloys have a single bcc phase, and for $x > 0.6$ they form a single fcc phase. But Ushida *et al* [29] have reported that by using a sputtering technique they were able to produce a single fcc phase for $x = 0.45$. In figure 3 we present the total DOS for the bcc phase ($x = 0.0$, 0.13, and 0.25) as well as the fcc phase ($x = 0.45$, 0.67, 0.92, and 1.0) of the $Fe_{1-x}Ag_x$ alloys (left-hand panel), along with the XPS results (right-hand panel). We note that the Fe d band and the Ag d band are well separated, indicating that $Fe_{1-x}Ag_x$ will be a split-band system. The band splitting is more than what we have seen in the case of $Fe_{1-x}Cu_x$, because the Ag d band lies at lower energy compared to the Cu d band (with respect to

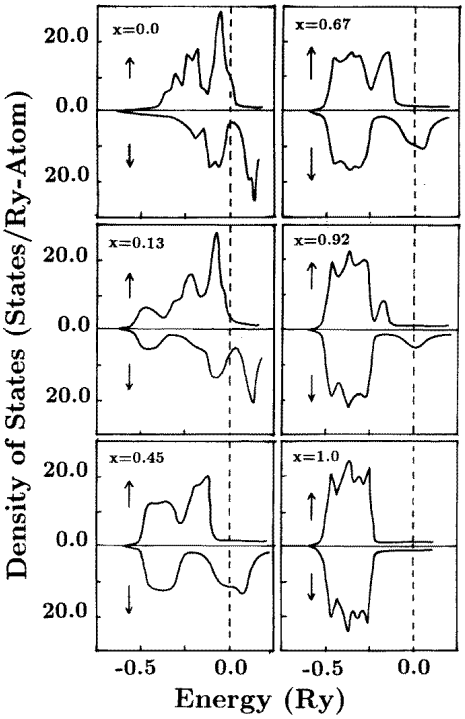

Figure 4. The spin-resolved density of states of $Fe_{1-x}Ag_x$ alloys for $x = 0.0$, 0.13, 0.45, 0.67, 0.92, and 1.0. The vertical dotted line indicates the Fermi level.

the corresponding Fermi energy) [43]. Again, our calculated DOS agree qualitatively with those of Kudrnovsky *et al* [38], and the XPS results corroborate our theoretical predictions. We also observe that, for this alloy, the DOS at E_F arises almost entirely from the Fe d bands. In figure 4 we show the spin-polarized DOS for this system, which are similar to those obtained by Kudrnovsky *et al* [38]. Again, as in the case of the $Fe_{1-x}Cu_x$ system, we observe that except for $x = 0.0$ (pure Fe) and $x = 1$, the major contribution to the total DOS at E_F is from the minority spins.

3.2. The magnetic moment

We have calculated the average magnetic moment of $Fe_{1-x}Cu_x$ and $Fe_{1-x}Ag_x$ alloys throughout the entire range of compositions, and compared our results with the available experimental data on the average magnetic moments of these alloys. In figure 5(a) we have plotted the average magnetic moments of the $Fe_{1-x}Cu_x$ alloys against the Cu concentration. We observe that our theoretical values of the magnetic moments for different concentrations are slightly larger than the corresponding experimental values as reported by Sumiyama *et al* [26]. The deviation is more towards the Cu-rich side of the alloy composition. Furthermore, experimentally, the magnetic moment vanishes at $x = 0.92$, whereas our theoretical calculations show that even for $x = 0.95$ the magnetic moment is non-zero, though it is very small. As local environmental fluctuations play an important role near the phase transition, we feel that this slight disagreement between the theory and experiment is probably due to the CPA, which does not take these fluctuations properly into account [44].

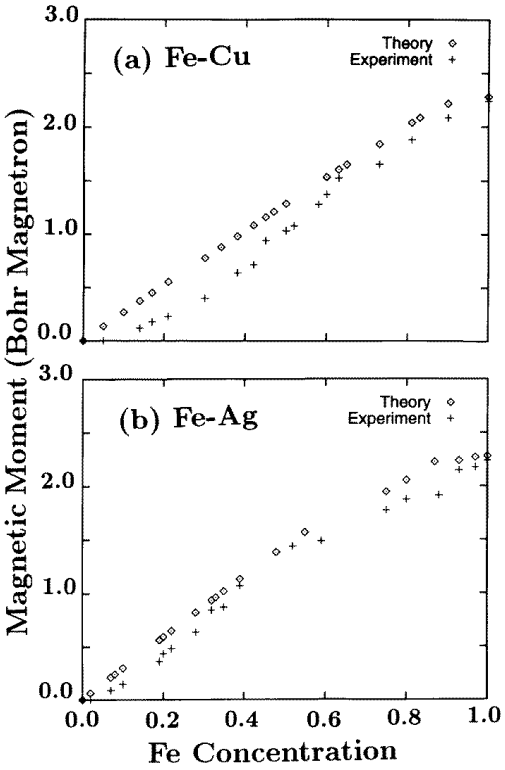

Figure 5. Theoretical (◇) (present work) and experimental (+) average magnetic moments of (a) $Fe_{1-x}Cu_x$ (the experimental results are after Sumiyama *et al* [26]) and (b) $Fe_{1-x}Ag_x$ (the experimental results are after Sumiyama and Nakamura [21]) alloys as functions of the composition.

However, we observe that there is an overall qualitative agreement between our theoretical results and the experimental results of reference [26]. Also, in a more recent publication, Ma *et al* [45] have reported that the magnetic moment of $Fe_{1-x}Cu_x$ alloys increases linearly with the Fe content, and there is no noticeable discontinuity at the fcc-to-bcc transition. Our theoretical results also show a similar trend.

In figure 5(b) we show the results for $Fe_{1-x}Ag_x$ alloys. In this case we find that there is even better agreement between our theoretical results and the experimental results of Sumiyama and Nakamura [21]. However, in this case also, we find that theory somewhat overestimates the value of the magnetic moment for all of the compositions of the alloy.

In figure 6(a) we show the theoretical values of the magnetic moments of an Fe atom for different compositions of $Fe_{1-x}Cu_x$ and $Fe_{1-x}Ag_x$ alloys. We note that the magnetic moment of an Fe atom in an Fe–Cu alloy for a particular composition is always lower than that of an Fe atom in an Fe–Ag alloy for the same composition. It has been earlier observed, both experimentally and theoretically, that Fe atoms in an alloy having a larger atomic volume tend to have a larger value of the magnetic moment than that in an alloy having a smaller atomic volume [46–49]. In a series of papers, Zeller, Dederichs, and co-workers [50–53] have presented the electronic structure and magnetic properties of dilute Fe alloys with transition metals and noble metals using the first-principles KKR Green's function method [50, 54]. They have reported similar observations. In the present case, we

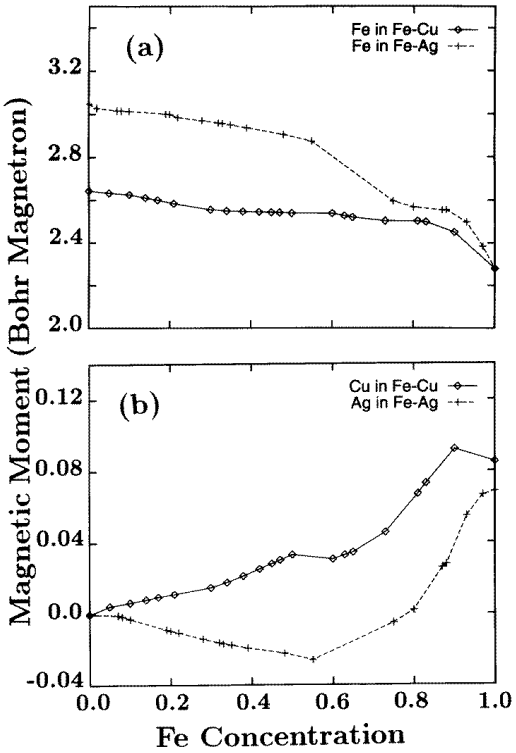

Figure 6. (a) The magnetic moments of an Fe atom in $Fe_{1-x}Cu_x$ ($\diamond$) and $Fe_{1-x}Ag_x$ (+) alloys for different compositions. (b) The magnetic moment of a Cu atom in $Fe_{1-x}Cu_x$ ($\diamond$) and that of a Ag atom in $Fe_{1-x}Ag_x$ (+) alloys for different compositions. The lines joining the points are a guide to the eye.

note that the lattice constant of Fe–Ag alloy is always larger than that of Fe–Cu alloy for the corresponding composition. Thus, our results corroborate the earlier observations on the ferromagnetic Fe alloys. The reason for the tendency towards larger magnetic moments in Fe–Ag alloys is that, due to the larger lattice constant of Fe–Ag alloys, the atomic behaviour of Fe atoms becomes more pronounced, and, therefore, the moments are always larger than in Fe–Cu alloys.

We also observe that the variation of the Fe magnetic moment with concentration is not significant in the Fe–Cu system, while it is considerable in the Fe–Ag system. This can be understood in terms of the Wigner–Seitz radii of the constituent atoms (Fe: 2.662 au; Cu: 2.669 au; Ag: 3.005 au), which are almost equal in the Fe–Cu system but quite different in the Fe–Ag system. In the Fe–Ag system, we observe a drop in the Fe moment at about $x = 0.65$. We note that at around this concentration the structure changes from fcc to bcc, and the Wigner–Seitz radii for fcc-$Fe_{0.55}Ag_{0.45}$ and bcc-$Fe_{0.75}Ag_{0.25}$ are 2.936 au and 2.747 au, respectively. Therefore, there is considerable change in the atomic volume while going from the fcc to the bcc phase, and this is responsible for the drop in the Fe magnetic moment. On the other hand, in the Fe–Cu system, the Wigner–Seitz radius does not vary significantly as a function of the composition, and hence we do not observe the above effect in this system.

For the sake of completeness, we have also shown the magnetic moments on Cu (Ag)

sites in Fe–Cu (Fe–Ag) alloys in figure 6(b). It is interesting to note that both Cu and Ag develop magnetic moments as a result of alloying with Fe, although the values are very small. This is to be expected because the electron gas in these alloys gets polarized as the ferromagnetism sets in.

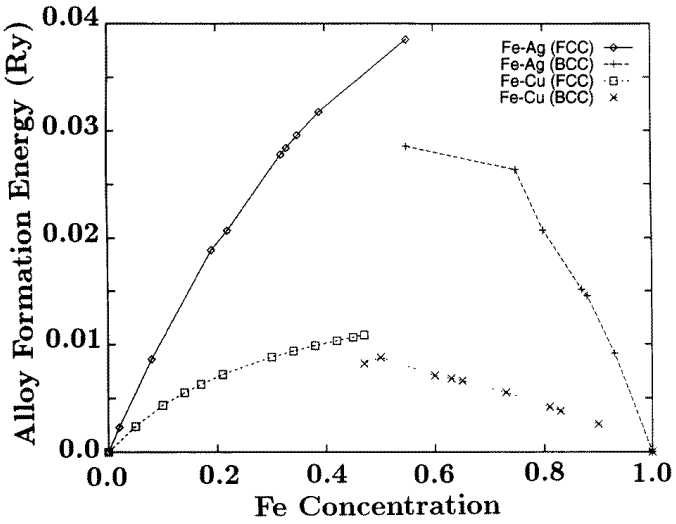

Figure 7. Alloy formation energy of fcc-$Fe_{1-x}Ag_x$ ($\diamond$), bcc-$Fe_{1-x}Ag_x$ ($+$), fcc-$Fe_{1-x}Cu_x$ ($\square$), and bcc-$Fe_{1-x}Cu_x$ ($\times$) alloys for different compositions. The solid lines joining the points are a guide to the eye.

3.3. The alloy formation energy

We have calculated the heat of formation or the alloy formation energy of the $Fe_{1-x}Cu_x$ and $Fe_{1-x}Ag_x$ alloys for different compositions. The results are shown in figure 7. We observe that the heat of formation is always non-negative, thereby implying the non-existence of a stable phase of these alloys. However, as reported in the literature, it is possible to overcome this barrier (positive heat of formation) by using special techniques, e.g. sputtering, and ion beam mixing. We also note that the heat of formation of the Fe–Ag alloys is much larger than that of the Fe–Cu alloys. This implies that the Fe–Ag alloys are more difficult to form than the Fe–Cu alloys. This agrees well with the experimental observations that, whereas one can produce Fe–Cu alloys at the terminal concentrations by solid quenching [19, 20], Fe and Ag are immiscible even in the liquid state [17, 21, 29].

4. Conclusions

We have presented the calculation of the DOS, magnetic moments, and heat of formation of Fe–Cu and Fe–Ag alloys using the first-principles TB-LMTO-CPA method. Our calculation of the DOS shows that these systems are split-band systems, in agreement with the XPS results. We find that the DOS is predominantly d-like at the Fermi energy. Our calculated magnetic moments are in good agreement with the experimental results. We find that Fe in Fe–Cu alloys has a lower magnetic moment than Fe in Fe–Ag alloys. We also find that

the heat of formation for these alloys is always positive, implying that these alloys cannot form stable phases under equilibrium conditions.

Acknowledgments

We thank Dr J Kudrnovsky for many helpful discussions and his help with the computer codes. SSAR also thanks Dr J B Staunton for helpful discussions. This research was supported by the Department of Science and Technology, New Delhi, India, through Grant SP/S2/M-39/87.

References

[1] Bansil A 1987 *Electronic Band Structure and its Applications* ed M Yussouff (Berlin: Springer) p 273
Bansil A 1993 *Z. Naturf.* a **48** 165
[2] Prasad R 1994 *Methods of Electronic Structure Calculations* ed O K Andersen, V Kumar and A Mookerjee (Singapore: World Scientific) p 211
[3] Andersen O K and Jepsen O 1984 *Phys. Rev. Lett.* **53** 2571
[4] Andersen O K, Jepsen O and Sŏb M 1987 *Electronic Band Structure and its Applications* ed M Yussouff (Berlin: Springer) p 1
[5] Andersen O K, Postnikov A V and Savrasov S Y 1992 *Applications of Multiple Scattering Theory to Materials Science (Materials Research Society Symposium Proceedings 253)* ed W H Butler, P H Dederichs, A Gonis and R L Weaver (Pittsburgh, PA: Materials Research Society) p 37
[6] Andersen O K, Jepsen O and Krier G 1994 *Methods of Electronic Structure Calculations* ed O K Andersen, V Kumar and A Mookerjee (Singapore: World Scientific) p 136
[7] For a review, see
von Barth U 1994 *Methods of Electronic Structure Calculations* ed O K Andersen, V Kumar and A Mookerjee (Singapore: World Scientific) p 21
[8] Kudrnovsky J and Masek J 1987 *Phys. Rev.* B **35** 2487
[9] Kudrnovsky J and Drchal V 1990 *Phys. Rev.* B **41** 7515
[10] Kudrnovsky J, Bose S K and Andersen O K 1991 *Phys. Rev.* B **43** 4613
[11] Kudrnovsky J 1994 *Methods of Electronic Structure Calculations* ed O K Andersen, V Kumar and A Mookerjee (Singapore: World Scientific) p 231
[12] Razee S S A and Prasad R 1993 *Phys. Rev.* B **48** 1361
[13] Mookerjee A and Prasad R 1993 *Phys. Rev.* B **48** 17 724
[14] Parkin S S P, Hopster H, Renard J P, Shinjo T and Zinn W (ed) 1992 *Magnetic Surfaces, Thin Films and Multilayers* (Pittsburgh, PA: Materials Research Society) p 231
[15] Falicov L M 1992 *Phys. Today* **45** (10) 46
[16] Ishikawa Y and Miura N (ed) 1991 *Physics and Engineering Applications of Magnetism* (Berlin: Springer)
[17] Kubaschewski O 1982 *Iron-Binary Phase Diagrams* (Berlin: Springer)
[18] Hansen M and Anderko K 1958 *Constitution of Binary Alloys* (New York: McGraw-Hill) p 20
Hansen M and Anderko K 1958 *Constitution of Binary Alloys* (New York: McGraw-Hill) p 580
[19] Aldred A T 1968 *J. Phys. C: Solid State Phys.* **1** 1103
[20] Window B 1972 *Phil. Mag.* **26** 681
[21] Sumiyama K and Nakamura Y 1984 *Phys. Status Solidi* a **81** K109
[22] Kneller E F 1964 *J. Appl. Phys.* **35** 2210
[23] Korn D and Pfeifle H 1976 *Z. Phys.* B **23** 23
[24] Kajzar F and Parette G 1979 *J. Appl. Phys.* **50** 1966
[25] Longworth G and Jain R 1978 *J. Phys. F: Met. Phys.* **8** 351
[26] Sumiyama K, Yoshitake T and Nakamura Y 1984 *J. Phys. Soc. Japan* **53** 3160
[27] Sumiyama K, Yoshitake T and Nakamura Y 1985 *Acta Metall.* **33** 1785
[28] Kataoka N, Sumiyama K and Nakamura Y 1985 *J. Phys. F: Met. Phys.* **15** 1405
[29] Ushida M, Tanaka K, Sumiyama K and Nakamura Y 1989 *J. Phys. Soc. Japan* **58** 1725
[30] Mazzone G and Antisari M V 1996 *Phys. Rev.* B **54** 441
[31] Window B 1970 *J. Phys. C: Solid State Phys.* **3** S325
[32] Gonser U, Meechan C J, Muir A H and Wiedersich H 1963 *J. Appl. Phys.* **34** 2373
[33] Gonser U, Grant R W, Meechan C J, Muir A H and Wiedersich H 1965 *J. Appl. Phys.* **36** 2124

[34] Gonser U, Grant R W, Muir A H and Wiedersich H 1966 *Acta Metall.* **14** 259
[35] For a review, see
Gonser U and Ron M 1980 *Applications of Mössbauer Spectroscopy* ed R L Cohen (New York: Academic) p 284 and references therein
[36] Chien C L, Liou S H, Kofalt D, Wu Yu, Egami T and McGuire T R 1986 *Phys. Rev.* B **33** 3247
[37] Kudrnovsky J, Bose S K and Andersen O K 1990 *J. Phys.: Condens. Matter* **2** 6847
[38] Kudrnovsky J, Bose S K and Andersen O K 1990 *J. Phys. Soc. Japan* **59** 4511
[39] von Barth U and Hedin L 1972 *J. Phys. C: Solid State Phys.* **5** 1629
[40] Hass K C, Velický B and Ehrenreich H 1984 *Phys. Rev.* B **29** 3697
[41] Drchal V, Kudrnovsky J and Weinberger P 1994 *Phys. Rev.* B **50** 7903
[42] Scofield J H 1976 *J. Electron Spectrosc. Relat. Phenom.* **8** 129
[43] Moruzzi V L, Janak J F and Williams A R 1978 *Calculated Electronic Properties of Metals* (New York: Pergamon)
[44] Staunton J B, Gyorffy B L, Johnson D D, Pinski F J, and Stocks G M 1989 *Alloy Phase Stability (NATO ASI Series B, vol 163)* ed G M Stocks and A Gonis (Dordrecht: Kluwer Academic) p 469 and references therein
[45] Ma E, Atzmon M and Pinkerton F E 1993 *J. Appl. Phys.* **74** 955
[46] Weiss R J 1963 *Proc. Phys. Soc.* **82** 281
[47] Shiga M 1972 *Solid State Commun.* **10** 1233
[48] Katsuki A and Terao K 1969 *J. Phys. Soc. Japan* **26** 1109
[49] Andersen O K, Madsen J, Poulsen U K, Jepsen O and Kollar J 1977 *Physica* B **86–88** 249
[50] Zeller R, Podloucky R and Dederichs P H 1980 *Z. Phys.* B **38** 165
[51] Podloucky R, Zeller R and Dederichs P H 1980 *Phys. Rev.* B **22** 5777
[52] Oswald A, Zeller R, Braspenning P J and Dederichs P H 1985 *J. Phys. F: Met. Phys.* **15** 193
[53] Drittler B, Stefanou N, Blügel S, Zeller R and Dederichs P H 1989 *Phys. Rev.* B **40** 8203
[54] Zeller R and Dederichs P H 1979 *Phys. Rev. Lett.* **42** 1713